

Tensile behaviour and fracture toughness of EPDM filled with untreated and silane-treated glass beads

D. ARENCÓN

Centre Català del Plàstic (CCP). Vapor Universitari de Terrassa. C/Colom 114, 08222 Terrassa, Spain

J. I. VELASCO*

*Departament de Ciència dels Materials i Enginyeria Metal·lúrgica, Escola Tècnica Superior d'Enginyers Industrials de Barcelona (ETSEIB), Universitat Politècnica de Catalunya (UPC). Avda. Diagonal 647, 08028 Barcelona, Spain
E-mail: jvelasco@cmem.upc.es*

The Essential Work of Fracture (EWF) theory has been applied to study the fracture behaviour of untreated and silane-treated glass bead-filled EPDM composites. The experimental values of both Young's modulus and tensile strength have been compared with those predicted by the main theoretical and semiempirical models, and the influence of the composite processing temperature on the tensile properties has been studied, noticing a marked drop of stiffness and strength from a processing temperature of 200 °C. A good adhesion between EPDM matrix and glass beads was achieved with the silane Z-6032, resulting in higher tensile strength, and it has been observed that glass bead presence induces plasticity in the EPDM matrix. No differences of the specific essential work of fracture were found in the three filled samples, although results show that the higher adhesion degree between matrix and particles, the higher value of the specific plastic work of fracture, and also the higher final instability in crack propagation. © 2001 Kluwer Academic Publishers

1. Introduction

The concept of the essential work of fracture (EWF) proposed by Broberg [1, 2] was first applied to metals in sheet form [3–8], paper grades like copy, sack paper and pulp handsheets [9–13]. Nowadays is becoming a useful way to characterise the fracture toughness of ductile polymers like PE, PP, PET, PETG, etc. [14–22] used in form of film for greenhouses or thin sheet for packaging applications.

The theory postulate that under plane-stress state the total fracture energy (W_f) of a notched specimen subjected to tensile loading could be divided into two parts: the essential work of fracture (W_e) and the non-essential or plastic work of fracture (W_p). The first one is associated with the instability on the crack tip, where the true process of fracture occurs, and is proportional to the specimen ligament; it is a work located in the so-called process inner zone. The second one refers to the plastic strain work and it is proportional to the volume of the outer process zone, which is just named plastic zone:

$$W_f = W_e + W_p = w_e l t + w_p \beta l^2 t \quad (1)$$

In the above general equation w_e and w_p are the specific essential and non-essential work of fracture re-

spectively, l the specimen ligament length, t the specimen thickness and β a shape factor related to the plastic zone geometry. Dividing the total work of fracture by the specimen ligament area the specific work of fracture can be obtained:

$$w_f = w_e + \beta w_p l \quad (2)$$

Thus, a linear relationship between the specific work of fracture and the specimen ligament length can be found, and therefore the specific essential work of fracture can be obtained when the ligament length is extrapolated to zero. The essential work of fracture is a material fracture parameter, ideally geometry independent, and even it has been proposed to be equivalent to the J-integral critical value (J_{IC}) [23]; however, the main contribution to the energy absorption during the fracture process of a ductile polymer sheet is the plastic strain, and so the non-essential term has to be also analysed. Usually, one can assure that a plane-stress state is in the fracture specimen if Hill's criterion [24] is satisfied, which establish for deeply double edge notched tension (DDENT) geometry that the maximum net stress (σ_{net}) possible to reach under plane-stress is 1.15 times the value of the uniaxial yield stress (σ_y) of the material. On the other

*Author to whom all correspondence should be addressed.

side, a pure plane strain state would be achieved when $\sigma_{net} = 2.97\sigma_y$ according to Hill's predictions. Although a few works have been published accounting for the application of EWF method to rubber toughened polymers [25], elastomeric PP [26] and ternary compounds of PP, SEBS and glass beads [27], the EWF should not be applicable to pure rubber materials, due to their reduced, almost null, contribution of plasticity to their fracture; so an elastic approach should be used. Nevertheless, we have observed that filling a thermoplastic elastomer (EPDM) with glass beads, a notorious contribution of plasticity can be observed before the fracture, being then possible to apply the EWF method to the fracture toughness characterisation of this kind of materials.

In this work, effort has been undertaken to study the fracture behaviour of binary composites consisting of EPDM elastomer and untreated and silane-treated glass beads, by means of EWF. Moreover, the influence of the processing temperature has been analysed on a basis of tensile properties.

2. Materials, compounding and specimens

A commercial EPDM (Dutral TER 4038), manufactured by Enichem, containing 27 wt% propylene, 68.5 wt% ethylene and 4.5 wt% 5-ethyliden-norbornene, was used as a matrix. Glass beads with an average particle size of $10\ \mu\text{m}$ were provided by Sovitec Ibérica, S.A. and silane coupling agents used for glass beads surface treatment were N-(2-(Vinylbenzyl-amino)-ethyl)-3-aminopropyltrimetoxysilane (Z-6032, Dow Corning) and a vinyl-based silane mixture (Ucarsil, Union Carbide). The general process carried out for filler surface treatment was as follows: A solution containing 30 ml of silane, 250 ml of methanol, 60 ml of water and 5 ml of acetic acid was prepared per each 1.5 kg of glass beads, and stirred for 20 minutes to assure the hydrolysis of the silane alkoxy groups, before the glass beads wetting. The treated glass beads were then dried in an oven at $60\ ^\circ\text{C}$ for 24 hours.

Compounding was performed using a *Collin* co-rotating twin-screw extruder. The screw diameter was 25 mm and its length to diameter ratio was 24. To study possible effects on the composite mechanical properties due to the processing temperature, compounding was carried out setting different die temperature: 115, 150, 180, 200, 220, $235\ ^\circ\text{C}$. In all cases the screw speed was fixed at 100 rpm. A good dispersion of the glass beads into the EPDM matrix was achieved by the following screw configuration: two compression zones on both sides of a mixing zone constituted by double-tipped kneading elements. A circular cross-section die of diameter 3-mm was adapted, and the extrudate was cooled in a water bath and pelletised. By this way three different compositions were prepared with filler nominal concentrations of 50% by weight, named B50, BUC50 and BZ50 for the untreated glass bead-filled EPDM and for surface-treated filled samples respectively. Unfilled EPDM was also subjected to the same extrusion process in order to get the same thermal and mechanical histories than the filled samples.

Plaques of nominal dimensions $150\ \text{mm} \times 150\ \text{mm} \times 2.5\ \text{mm}$ and $150\ \text{mm} \times 150\ \text{mm} \times 1.3\ \text{mm}$ were com-

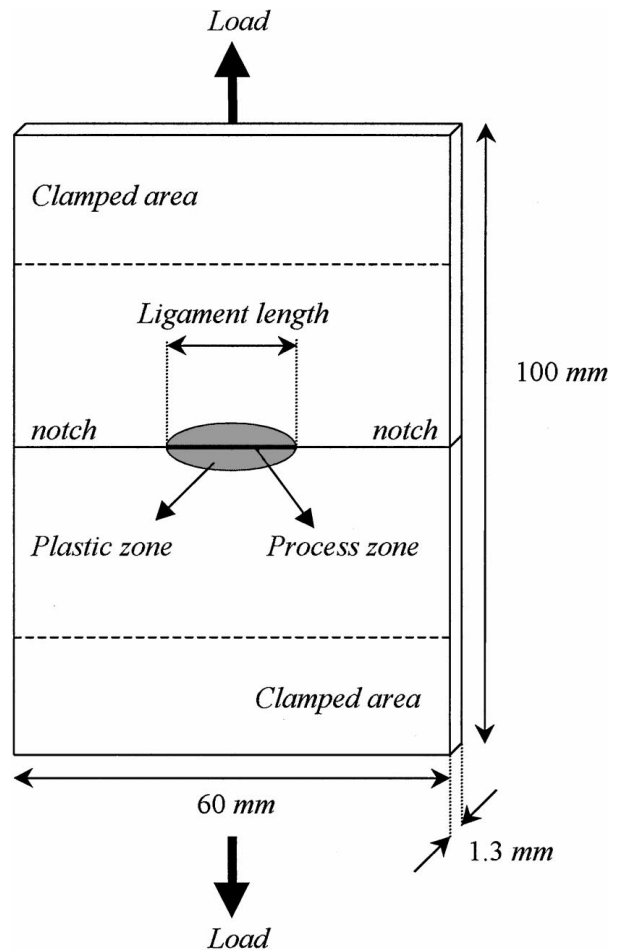


Figure 1 DDENT specimen geometry used in the EWF tests.

pression moulded with a hot plate press at $115\ ^\circ\text{C}$, applying a maximum pressure of 100 bar and cooling under pressure to room temperature. Two types of test specimens were obtained with these plaques. By one hand, dumbbell-shaped specimens (type C according ASTM D-412 [28]) were cut off to carry out the tensile characterisation and, by the other hand, DDENT specimens (Fig. 1) were sawn from the 1.3 mm thick plaques for fracture testing. The notches were made with a razor blade, and the ligament length was measured employing a travelling microscope.

3. Testing

3.1. Tensile tests

Tensile tests were performed at a crosshead speed of 100 mm/min and at room temperature using a universal testing machine (Adamel DY-30), provided with a load cell of 100 N and equipped with a laser extensometer (Hounsfield 500-L). At least five specimens were tested per each compound and processing temperature. The obtained values of Young's modulus (E) and the tensile strength (stress at a strain of 200%) have been used to investigate the influence of the surface treatment of the particles and the compounding temperature.

3.2. Fracture tests

The EWF method was applied to the materials processed at $115\ ^\circ\text{C}$ on the above-described DDENT specimens. All the tests were performed at a crosshead speed of 10 mm/min at room temperature. At least thirteen

specimens of each material were tested, having different ligament length ranging from 3 to 20 mm according to the ESIS protocol [29]. The load/displacement curve was integrated to obtain the total energy absorbed by the sample during the fracture process, and the maximum load value was used to check Hill's criterion.

3.3. Fractography

To investigate the morphological aspects associated with the fracture process, the fracture surfaces were examined by scanning electronic microscopy (SEM), using a *Jeol JSM-820* equipment, after coating the samples with a thin gold layer. Moreover, optical microscopy was used to measure the specimen plastic zone.

4. Results and discussion

4.1. Tensile behaviour

Rubber typical tensile behaviour has been observed, and two different ranges of strain can be distinguished to analyse the mechanical characteristics of these materials (Fig. 2). Firstly, we can distinguish a low-strain elastic regime, from which was possible to obtain the Young's modulus (Table I).

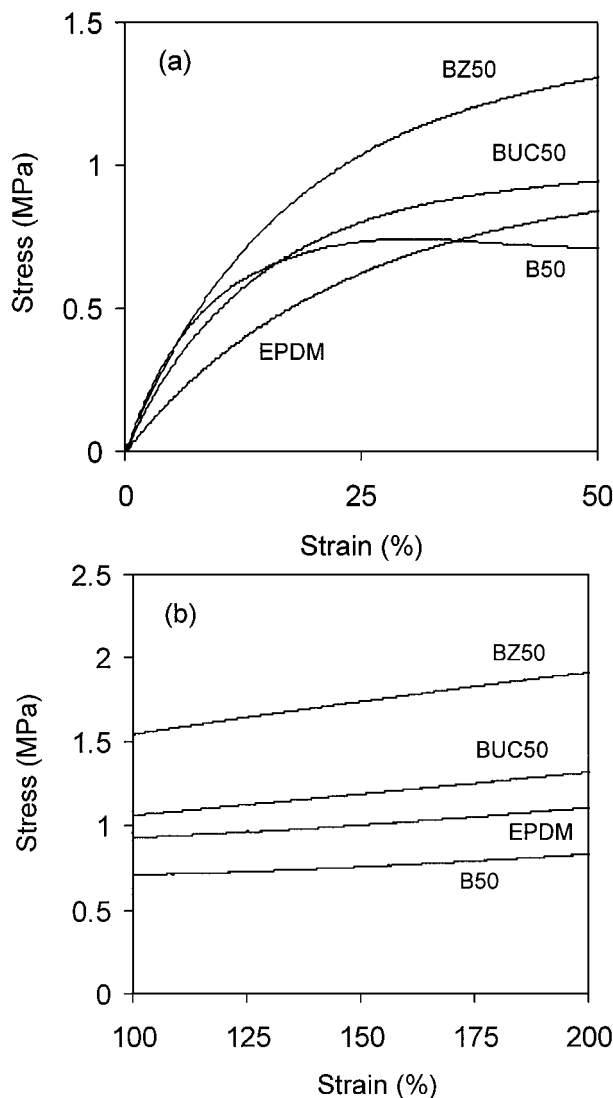


Figure 2 Stress/strain tensile curves of the studied materials; (a) range of small strain, (b) range of high strain.

TABLE I Numerical results of tensile characterisation carried out at 100 mm/min for all the materials and processing temperatures

Sample	Extrusion die temperature (°C)	Young's modulus, E (MPa)	Tensile strength, $\sigma_{200\%}$ (MPa)
EPDM	115	3.79 ± 0.66	1.07 ± 0.02
	150	4.10 ± 0.58	0.99 ± 0.03
	180	3.66 ± 0.81	1.02 ± 0.05
	200	3.76 ± 0.66	0.93 ± 0.01
	220	3.26 ± 0.03	1.13 ± 0.08
	235	1.87 ± 0.06	0.89 ± 0.07
B50	115	7.67 ± 0.73	1.25 ± 0.04
	150	6.27 ± 0.43	0.76 ± 0.04
	180	7.75 ± 0.45	0.84 ± 0.04
	200	7.12 ± 0.40	0.79 ± 0.02
	220	4.83 ± 0.01	0.86 ± 0.05
	235	3.48 ± 0.03	—
BUC50	115	7.62 ± 0.43	1.28 ± 0.17
	150	6.13 ± 1.21	1.24 ± 0.06
	180	6.36 ± 0.64	1.14 ± 0.01
	200	7.23 ± 0.74	1.05 ± 0.08
	220	5.65 ± 0.48	0.99 ± 0.04
	235	4.83 ± 0.38	0.72 ± 0.08
BZ50	115	8.19 ± 0.44	2.00 ± 0.01
	150	7.31 ± 0.35	1.89 ± 0.05
	180	8.19 ± 0.44	1.61 ± 0.08
	200	7.05 ± 0.75	1.75 ± 0.06
	220	5.36 ± 0.67	1.49 ± 0.03
	235	4.69 ± 0.28	1.09 ± 0.04

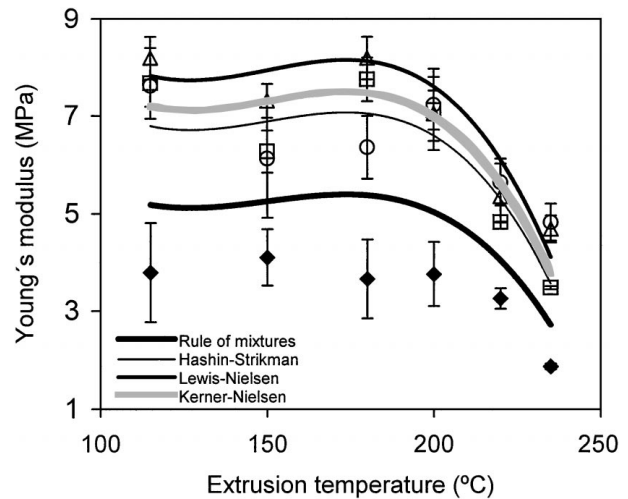


Figure 3 Comparison of experimental Young's modulus with predicted values, as a function of the extrusion temperature. (◆) EPDM, (□) B50, (○) BUC50 and (△) BZ50.

As expected, filling the EPDM results in higher material stiffness, but no differences were appreciated between silane-treated and non-treated glass bead filled samples. Moreover, Young's modulus remained constant when the temperature extrusion was increased until 200 °C approximately, however, increasing the temperature extrusion above this value, a remarkable drop in Young's modulus is observed, what could be explained on the basis of matrix degradation (Fig. 3).

From the stress/strain curves, one can observe that whereas unfilled EPDM did not display a definite yield point, EPDM filled with untreated glass did it. The rubbery character of unfilled EPDM make the material

be deformed mainly elastically, but when glass beads are present, these ones could be easily debonded from matrix, giving a clear yield point on the curve. In this sense, if glass beads were strongly bounded to EPDM, the composite could show a deformation pattern similar to the unfilled EPDM, that is, without a yield point, because in this case the viscous phenomena (matrix debonding) located at the interface would be constrained. BUC50 and BZ50 samples seemed to agree with this behaviour.

In order to get information about tensile strength at high strain levels, the stress value at 200% of strain have been compiled (Table I). It can be observed that filled EPDM with untreated glass beads showed lower strength than pure EPDM, whereas samples filled with silane-treated glass beads gave higher values, particularly BZ50 sample (Fig. 2b). This results in an evidence of improved adhesion promoted by Z-6032 silane, which is acting generating an effective interface to transmit stress between matrix and glass beads. In contrast, when untreated glass bead filled EPDM is highly strained, its effective cross-section area is reduced due to particle debonding, and so its tensile strength is reduced too.

Several theoretical and semiempirical models are usually used for predicting the Young's modulus of particulate filled polymers [30–32], and have also been used in this work to compare predicted values with experimental ones. Most of these equations are derived from Kernel's model [33], which consists of dispersed spheres into a matrix and perfectly bounded to it. From a distance of each inclusion, the material is supposed to have homogeneous properties, whereas at the interface the properties change gradually from those of the particles to those of the matrix. Nielsen adapted the elastic properties derived by Kerner to make easy its practical application to the Young's modulus prediction of spherical particulate filled materials. Kerner-Nielsen [34] equation is expressed as:

$$E_c = E_m \left(\frac{1 + AB\phi_f}{1 - B\phi_f} \right) \quad (3)$$

with

$$A = \frac{7 - 5\nu_m}{8 - 10\nu_m} \quad (4)$$

and

$$B = \frac{E_f/E_m - 1}{E_f/E_m + A} \quad (5)$$

being ϕ_f the filler volume fraction, and E_c , E_m and E_f the Young's modulus of composite, matrix and filler respectively. In our case E_f has been taken equal to 68600 MPa and the matrix Poisson ratio (ν_m) equal to 0.4999 [35]. Lewis and Nielsen [36] incorporated to the Equation 3 an additional factor, ψ , which depends on the filler volume fraction of maximum packaging, ϕ_f^{\max} [37–39]:

$$E_c = E_m \left(\frac{1 + AB\phi_f}{1 - B\psi\phi_f} \right) \quad (6)$$

Assuming isostress conditions, values predicted by the well-known rule of mixtures have also been compared with the experimental results, and also the Hashin-Strikman equation [40] has been checked:

$$G_c = G_m + \frac{\phi_f}{\frac{1}{G_f - G_m} + \frac{6(K_m + 2G_m)(1 - \phi_f)}{5G_m(3K_m + 4G_m)}} \quad (7)$$

Where G_m , G_f and G_c are the shear modulus of matrix, filler and composite respectively, and K_m , is the matrix bulk modulus. In this case, Young's modulus is obtained from the basic relationship of elasticity:

$$E = 2G(1 + \nu) \quad (8)$$

As it can be observed in Fig. 3, results indicate that checked equations (which have been derived assuming isostress conditions in the composite) could predict quite well Young's modulus values for these materials, with the exception of the rule of mixtures. Differences found in predictions of E_c employing these models are lower than differences found between the experimental Young's modulus values.

Concerning to the composite tensile strength, the Nicolais-Narkis equation [41] is usually used to predict the tensile strength of a material containing spherical inclusions:

$$\sigma_c = \sigma_m(1 - 1.21\phi_f^{2/3}) \quad (9)$$

Nevertheless, another equation can be considered for taking into account the interfacial adhesion, through the value of the interfacial shear strength (τ):

$$\sigma_c = \sigma_m(1 - \phi_f) + 2\frac{l}{d}\tau\phi_f \quad (10)$$

Equation 10 is usually used to predict the tensile strength of polymers filled with fibres shorter than the critical length. To adapt it to our case, the fibre aspect ratio (l/d) was taken equal to one.

As shown in Fig. 4, the tensile strength of these materials could not be well predicted by the Nicolais-Narkis

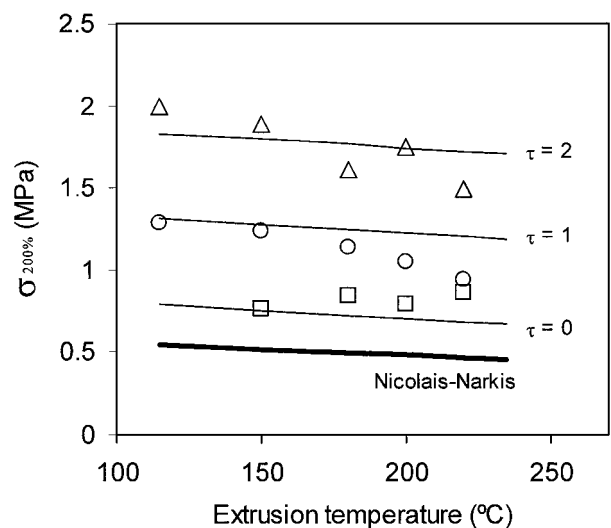


Figure 4 Comparison of experimental tensile strength with predicted values by Nicolais-Narkis equation and interfacial shear strength-based model. Symbols like in Fig. 3.

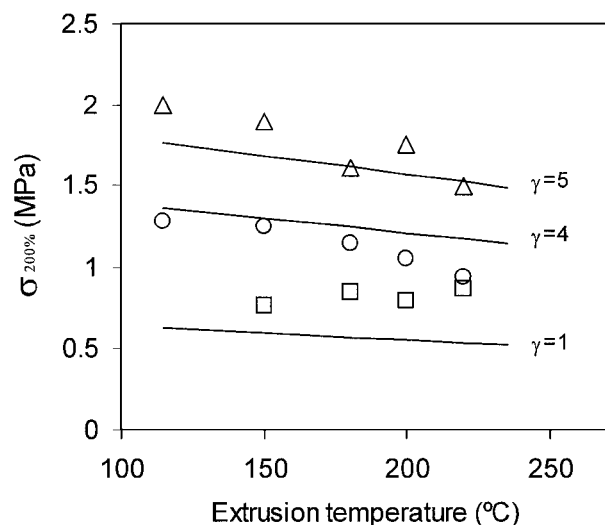


Figure 5 Comparison of experimental tensile strength with predicted values of Pukzanszky equation, for different value of γ parameter. Symbols like in Fig. 3.

equation, and a model accounting for interface properties seems to be more accurate. In this sense, the application of equation 10 resulted in a value of the interfacial shear strength close to 2 MPa for BZ50 sample, and it was almost zero for B50 sample as expected from differences in interfacial adhesion between EPDM and untreated and silane-treated glass beads.

Another way of evaluating the interfacial adhesion was developed by Pukzansky [42], who established the next equation:

$$\sigma_c = \sigma_m \frac{1 - \phi_f}{1 + 2.5\phi_f} \exp(\gamma\phi_f) \quad (11)$$

Where γ is a parameter related with the interface properties such as thickness and shear strength, and give us information about the capacity of the interface for transmitting stresses between phases. As displayed in Fig. 5, the higher value of γ are found for BZ50, showing again this sample an improved adhesion between glass beads and EPDM matrix with respect to B50 and BUC50.

4.2. Essential work of fracture

The specific work of fracture (w_f) was calculated from the area under the load/displacement curve recorded in the fracture test (Fig. 6), and it has been plotted against the specimen ligament length in Figs 7 and 8 in order to find w_e and w_p values. As expected, unfilled EPDM did not display linearity between w_f and l values (Fig. 7), and consequently the EWF theory could not be applied. In this material the viscous phenomena occurring under tensile loading are negligible and there was no evidence of plastic zone developed before crack growth initiation. In the opposite, the presence of glass bead in EPDM promoted viscous phenomena at the interface, mainly consisting in glass bead debonding. As a result, a plastic zone is developed in these filled samples before the fracture onset, and a good linearity of points can be appreciated in the w_f against l plots (Fig. 8). In these samples, after the plastic zone is formed around the specimen ligament, crack propagation goes

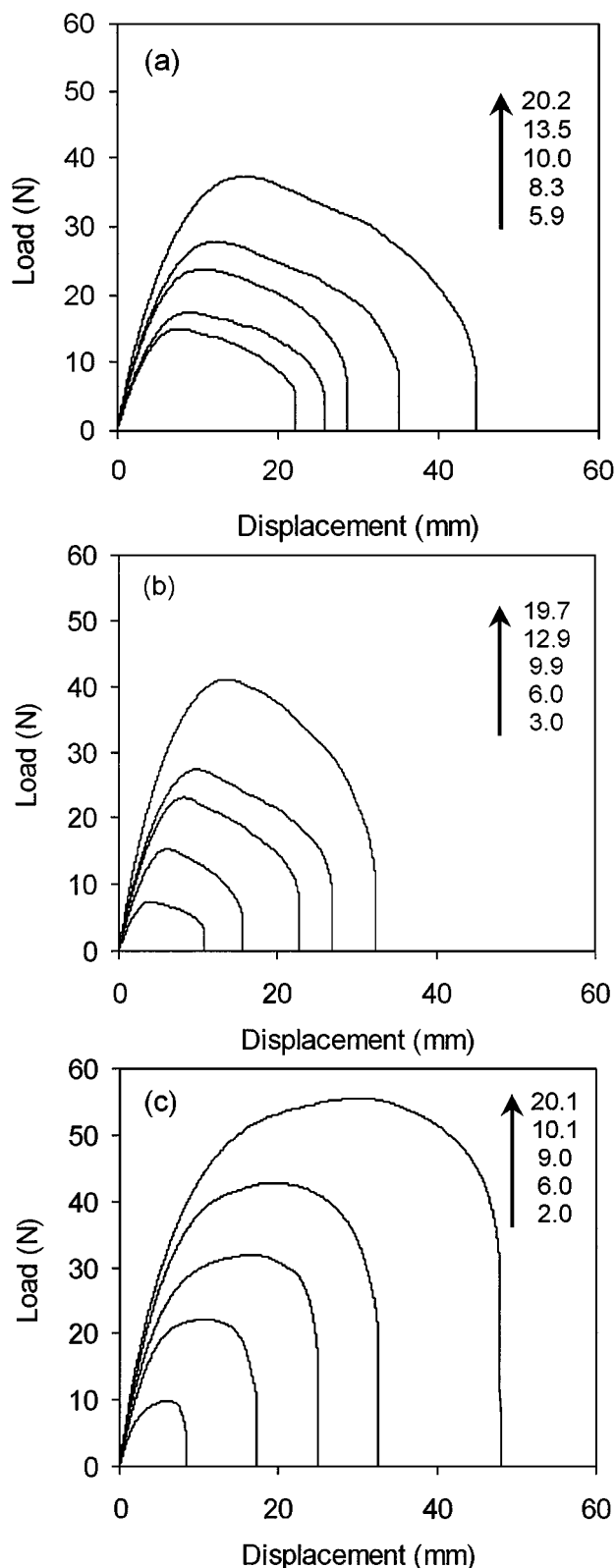


Figure 6 Plots obtained from EWF tests for (a) B50, (b) BUC50 and (c) BZ50. Numbers beside arrow indicate the ligament length values (mm) of the shown curves.

through a general mechanism of EPDM stable ductile tearing.

To determine the specific plastic work of fracture (w_p) an average value of the shape factor (β) had to be calculated for each material. The shape of the plastic zone developed around the specimen ligament length was elliptical in all cases (Fig. 9) and, according to this shape, β was measured in each tested specimen [29].

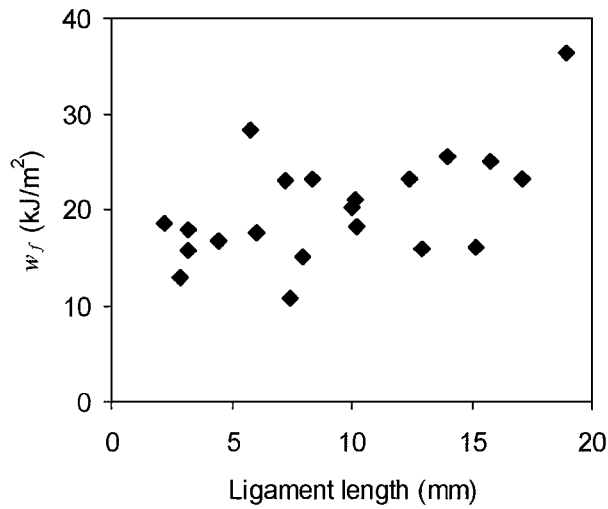


Figure 7 Application of EWF method to unfilled EPDM, showing no data linearity.

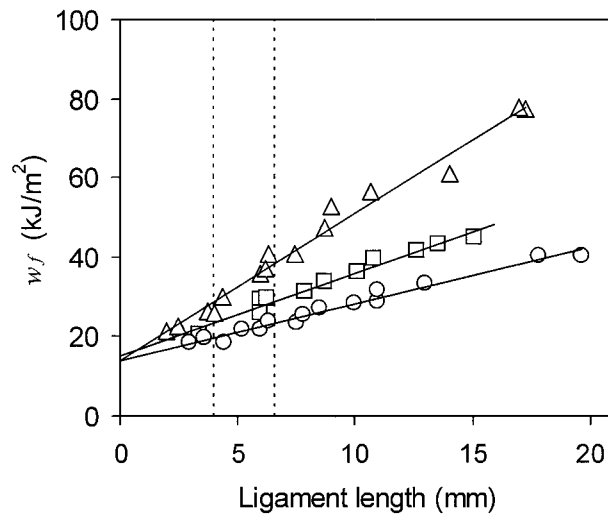


Figure 8 Linearisation of the specific work of fracture for filled EPDM. The zone comprised between dashed lines indicates the ligament length range where the stress state transition is usually observed. Symbols like in Fig. 3.

The ellipse minor axis was found to decrease as follows B50 > BUC50 > BZ50, which indicates that interfacial adhesion limit the viscous phenomena, resulting in a reduced area of the plastic zone.

The obtained values of the EWF parameters have been compiled in Table II. By one hand, the resulting higher value of w_p in BZ50 sample indicates that this material consumes more energy during the plastic deformation process previous to the crack propagation onset than the other two filled samples, which must be a direct consequence of its higher tensile strength promoted by interfacial adhesion. Also, although BUC50 material presented the lower values of specific work of fracture (w_f), it results in a similar value of the specific

TABLE II Fracture parameters obtained from EWF application

Sample	w_e (kJ/m ²)	β	w_p (MJ/m ³)
B50	15.56	0.310	6.67
BUC50	14.14	0.212	6.84
BZ50	14.04	0.177	20.92

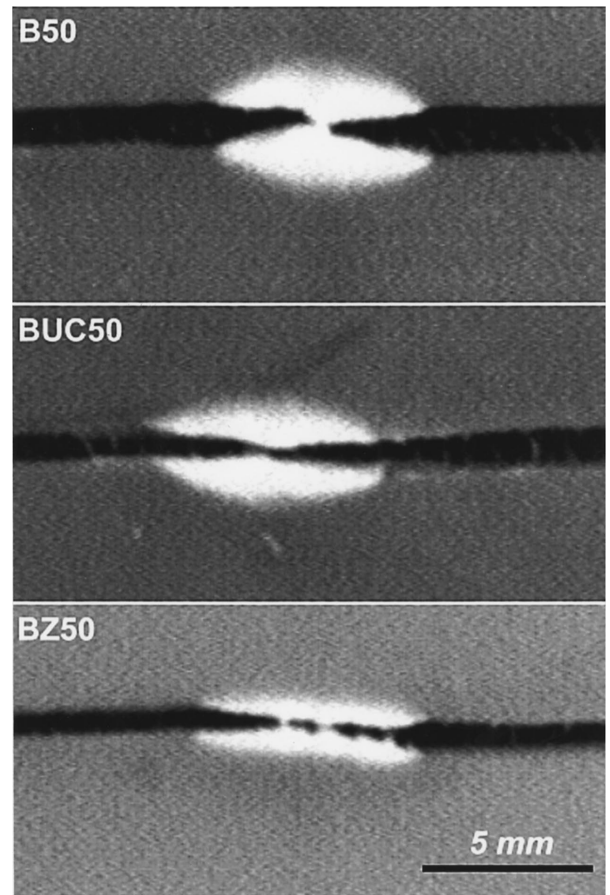


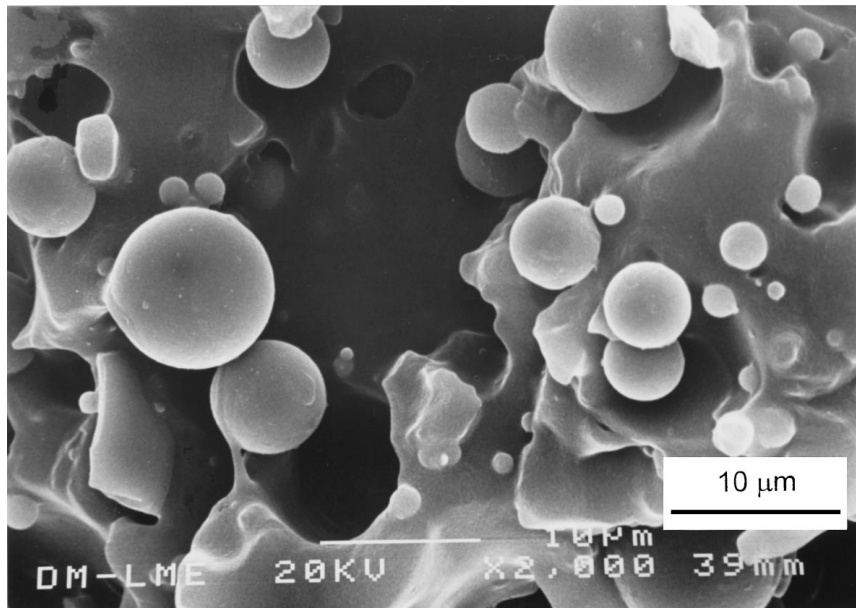
Figure 9 Photographs showing the plastic zone developed in fractured DDENT specimens.

plastic work (w_p) than B50 sample, which is due to its lower shape factor.

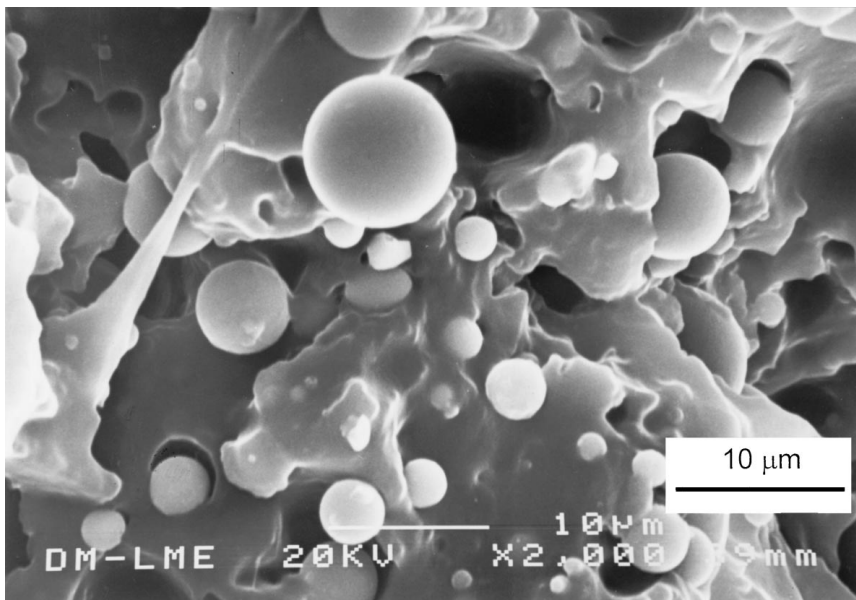
By the other hand, the obtained values of w_e do not show significant differences between the three filled materials, what indicates that interfacial adhesion has no influence on the essential work of fracture. In other words, crack propagates mainly through the EPDM matrix in all these samples.

The observation of the fracture surfaces by SEM seems to confirm the explanation given to the results, which is related to differences of interfacial adhesion between glass beads and EPDM. This polymer exhibits no practical adhesion with untreated glass beads, which is displayed by SEM as glass bead smooth surfaces (Fig. 10a). Also, although the tensile strength of BUC50 was slightly higher than B50 there is no microscopic evidence of better adhesion in this case (Fig. 10b). Nevertheless, no doubt of a good adhesion was found in composite BZ50, noticing by SEM rough particle surfaces and partial embedding by the EPDM matrix (Fig. 10c).

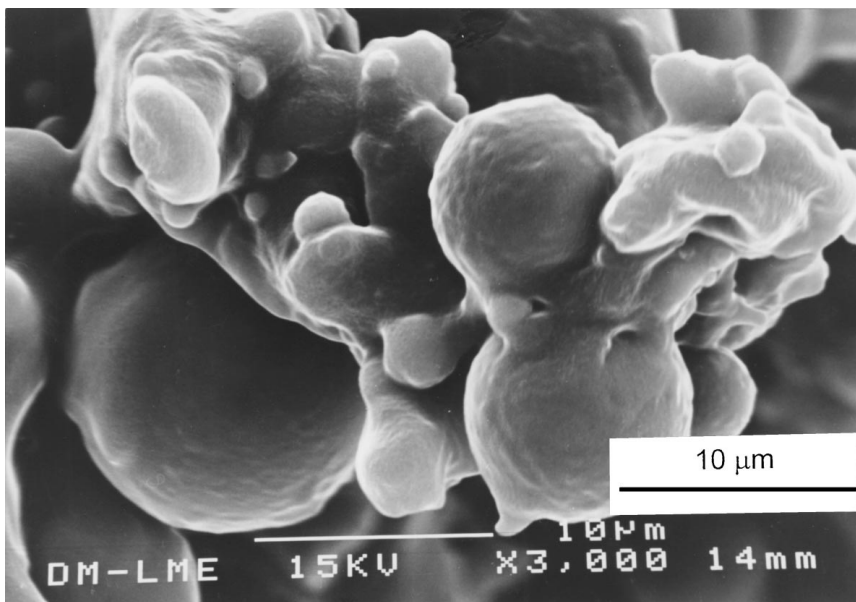
In order to verify if the obtained values of the specific essential work of fracture agree with those of plane stress, plane strain or mixed state of stress, Hill's criterion has been checked. For this purpose, σ_{net} values have been compared in Fig. 11 with those predicted by Hill [24] for pure plane stress and plane strain conditions ($1.15\sigma_y$ and $2.97\sigma_y$ respectively). Values of σ_y were obtained from tensile test carried out at 100 mm/min on the dumbbell-shaped specimens. Assuming the possible error made on the yield stress determination, plots of Fig. 11 indicate that the three filled materials are



(a)



(b)



(c)

Figure 10 Micrographs of fracture surfaces by SEM, showing different adhesion degree between EPDM matrix and glass beads, for (a) B50, (b) BUC50 and (c) BZ50.

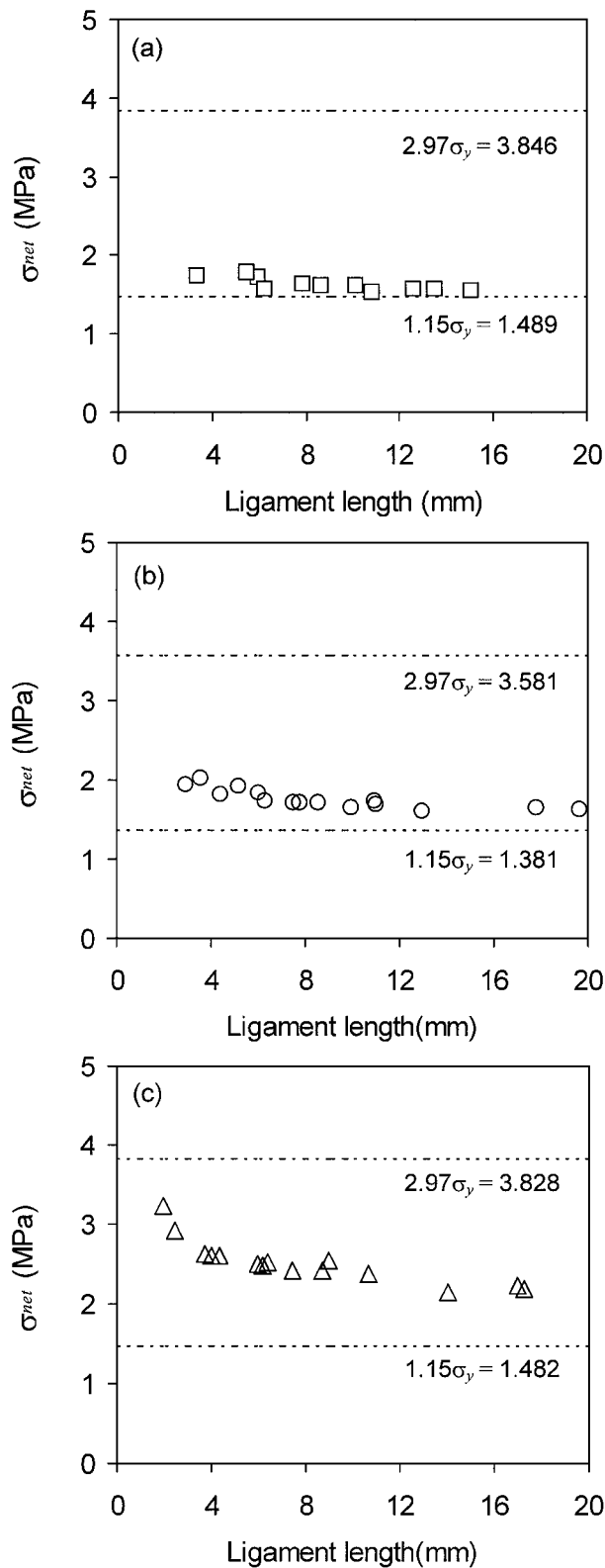


Figure 11 Maximum net stress values in comparison with Hill's predictions for (a) B50, (b) BUC50 and (c) BZ50. Dashed lines represent the stress values for pure plane stress and pure plane strain according to Hill.

under a mixed mode of stress, although σ_{net} values of BUC50 and specially B50 sample are close to $1.15\sigma_y$. The following criterion, which is usually used to assess plane strain conditions, has been also checked: $t \geq 25 (w_e/\sigma_y)$. In the three samples t values have been found to be much higher than the specimen thickness value (1.3 mm), indicating again no pure plane strain state.

It is noticeable that crack propagation in these materials goes through a two-step process. Firstly, crack propagates through stable ductile tearing, however crack growth instability finally occurs, which is displayed as a sudden drop of the load value in plots of Fig. 6. Such final instability is found to be more intense as higher is the interfacial adhesion degree in the filled sample ($BZ50 > BUC50 > B50$), and it seems to be provoked by the plane strain contribution to the material stress state. So, BZ50 sample would be under a higher contribution of plane strain into the mixed mode of stress, giving the instability at the higher load values, whereas B50 sample would be near to a pure plane stress state, as explained before on a basis of Hill's criterion. Consequently, if differences in the stress state of the three materials are assumed, the obtained values of w_e should be taken carefully.

5. Conclusions

Glass bead-filled EPDM composites (50/50) were compounded and studied focusing on tensile and fracture behaviour through EWF method. A good interfacial adhesion between EPDM and glass beads was achieved by means of treatment with silane Z-6032 and, as a result, BZ50 sample showed the higher tensile strength.

Composite Young's modulus was found to be well predicted by the main equations based in isostress conditions, and two models accounting for the interfacial shear strength were found to be right to predict the tensile strength of these materials. Above an extrusion temperature of 200 °C a remarkable fall in the tensile properties could be observed in these materials.

Whereas EWF theory could not be applied to unfilled EPDM, due to its lack of plasticity, the glass bead presence promoted quite plasticity in this material and thus the fracture behaviour of filled EPDM samples could be studied by means of the EWF concept. It was found that the strength of the interface, which could be varied through glass surface treatment with silane, played an important role in the composite fracture behaviour. Firstly, the higher adhesion degree, the higher specific plastic work of fracture, due to a higher tensile strength. Secondly, although no remarkable differences of the specific essential work of fracture (w_e) were found between the three filled materials (which would be due to a common mechanism of crack growth through the EPDM matrix) the higher adhesion degree at the interface resulted in a higher contribution of plane strain to the material stress state. This resulted in more intense final crack propagation instability in the sample with better adhesion (BZ50).

Acknowledgements

Financial assistance from CIRIT (D. Arencón) is gratefully acknowledged. We also thank Enichem Ibérica, Sovitec Ibérica, Dow Corning and Union Carbide for supplying EPDM, glass beads, and silanes respectively.

References

1. K. B. BROBERG, *Int. J. Fracture* **4** (1968) 11.
2. *Idem.*, *J. Mech. Phys. Solids* **23** (1975) 215.
3. B. COTTERELL and J.K. REDDEL, *Int. J. Fracture* **13** (1977) 267.

4. Y. W. MAI and B. COTTERELL, *J. Mater. Sci.* **15** (1980) 2296.
5. A. H. PRIEST and B. HOLMES, *Int. J. Fracture* **17** (1981) 277.
6. Y. W. MAI and B. COTTERELL, *Eng. Fract. Mech.* **21** (1985) 123.
7. *Idem.*, *Int. J. Fracture* **30** (1986) R37.
8. M. P. WUNK and D. T. REED, *ibid.* **31** (1986) 161.
9. B. COTTERELL and Y. W. MAI, "Advances in Fracture Research" (Pergamon Press, Oxford, 1981) p. 1683.
10. R. S. SETH, G. ROBERTSON, Y. W. MAI and J. D. HOFFMANN, *Tappi* **76** (1993) 109.
11. R. S. SETH, *ibid.* **79** (1995) 177.
12. Y. W. MAI, H. HE and R. LEUNG, *Fracture Mechanics: ASTM STP* **26** (1995) 587.
13. R. S. SETH, *Tappi* **79** (1996) 170.
14. A. S. SALEEMI and J. A. NAIRN, *Pol. Engng. Sci.* **30** (1990) 211.
15. Y. W. MAI and P. POWELL, *J. Polym. Sci. (Polym. Phys.)* **29** (1991) 785.
16. W. F. CHAN and J. G. WILLIAMS, *Polymer* **35** (1994) 1666.
17. J. WU and Y. W. MAI, *Polym. Engng. Sci.* **36** (1996) 2275.
18. S. HASHEMI, *J. Mater. Sci.* **32** (1997) 1563.
19. M. LL. MASPOCH, O. O. SANTANA, J. GRANDO, D. FERRER and A. B. MARTÍNEZ, *Polym. Bull.* **39** (1997) 249.
20. J. KARGER-KOCSIS, T. CZIGÁNY and E. J. MOSKALA, *Polymer* **38** (1997) 4587.
21. *Idem.*, *ibid.* **39** (1998) 3939.
22. D. FERRER-BALAS, M. LL. MASPOCH, A. B. MARTÍNEZ and O. SANTANA, *Polym. Bull.* **42** (1999) 101.
23. Y. W. MAI and B. COTTERELL, *J. Mater. Sci.* **15** (1980) 2296.
24. R. HILL, *J. Mech. Phys. Solids* **1** (1952) 19.
25. A. PEGORETTI, A. MARCHI and T. RICCO, *Polym. Engng. Sci.* **37** (1997) 1045.
26. D. E. MOUZAKIS, M. GAHLEITNER and J. KARGER-KOCSIS, *J. Appl. Polym. Sci.* **70** (1998) 873.
27. D. E. MOUZAKIS, F. STRICKER, R. MÜLHAUPT and J. KARGER-KOCSIS, *J. Mater. Sci.* **33** (1998) 2551.
28. ASTM D412, 1998.
29. Test Protocol for Essential Work of Fracture, European Structural Integrity Society (ESIS), October 1997.
30. P. S. THEOCARIS and E. SIDERIDIS, *J. Appl. Pol. Sci.* **29** (1984) 2997.
31. M. E. J. DEKKERS and D. HEIKENS, *ibid.* **30** (1985) 2389.
32. A. MEDDAD and B. FISA, *J. Mater. Sci.* **32** (1997) 1177.
33. E. H. KERNER, *Proc. Phys. Soc. (B)* **69** (1956) 802.
34. L. E. NIELSEN, *J. Appl. Phys.* **41** (1979) 4626.
35. D. L. HERTZ JR., in "Engineering with Rubber: How to Design Rubber Components," edited by Alan N. Gent. (Carl Hanser Verlag, Munich, 1992) p. 4.
36. T. B. LEWIS and L. E. NIELSEN, *J. Appl. Pol. Sci.* **14** (1970) 1449.
37. A. M. RILEY, C. D. PAYNTER, P. M. MC GENITY P. M. and J. M. ADAMS, *Plast. Rubb. Proc. Appl.* **14** (1990) 85.
38. J. JANCAR, *J. Mater. Sci.* **24** (1989) 3947.
39. *Idem.*, *ibid.* **24** (1989) 4268.
40. Z. V. I. HASHIN and S. STRIKMAN, *J. Mech. Phys. Solids* **11** (1963) 127.
41. L. NICOLAIS and M. NARKIS, *Pol. Engng. Sci.* **11** (1971) 194.
42. B. PUKÁNSZKY, *Polym. Comp.* **21** (1990) 255.

Received 30 July 1999
and accepted 5 April 2000